

Special Draft Technical Memorandum

Design, Operation, and Calibration of a Shipboard Fast Rotating Shadowband Spectral Radiometer

28 Aug 1998

NASA SIMBIOS Contract #52-210.91
Validation of the SeaWiFS Atmospheric Correction Scheme
Using Measurements of Aerosol Optical Properties

R. Michael Reynolds, Mark A. Miller, and Mary J. Bartholomew
Brookhaven National Laboratory
reynolds@bnl.gov

1. Instrument Description

The Brookhaven National Laboratory (BNL) has developed a ship-board shortwave radiation instrument platform called the Portable Radiation Package (PRP) (Figure 1). The PRP is composed of a broadband Precision Spectral Pyranometer (PSP) made by Eppley Laboratory, Inc., a fast-rotating shadowband (FRS) spectral radiometer, which is the subject of this paper, attitude sensors for the measurement of platform pitch, roll, and azimuth, and a special microprocessor for data collection and instrument control.

The FRS spectral radiometer (Figure 2) is designed to provide quality estimates of direct and diffuse shortwave irradiance from a moving platform without need of special gyro-stabilized tables. It is small, environmentally robust, low power, and is well suited for research ships, for ice floes, or for larger buoys in all but the higher Beaufort conditions.

The arm rotational speed is 5.5 sec per revolution, meaning the arm moves across the upper hemisphere, relative to the sensor, in 2.25 sec. The hemispherical shape of the arm ensures that the sensor will see a shadow, regardless of its azimuth heading. The arm moves across the face of the sun in a few tenths of a second and the head is in full shadow for about one tenth of a second.

Spectral irradiance measurements are made with a modified spectral radiometer head (Yankee Environmental Systems, Inc.). The head has seven detectors (channels), a broadband channel and six 10 nm bandpass measurements at 330, 415, 490, 550, 650, and 960 nm. It can be accurately calibrated and has an excellent zenith angle response. The head construction, adeptly described by Harrison et al. (1994), is environmentally sound and the package is weatherproof, robust, and suitable for use in a marine environment. Figure 3 shows a typical solar spectrum at the top of the atmosphere and at the Earth's surface. Superimposed on the graph are the pass bands of the silicon cell photo diode and the six FRS spectral radiometer narrowband channels.

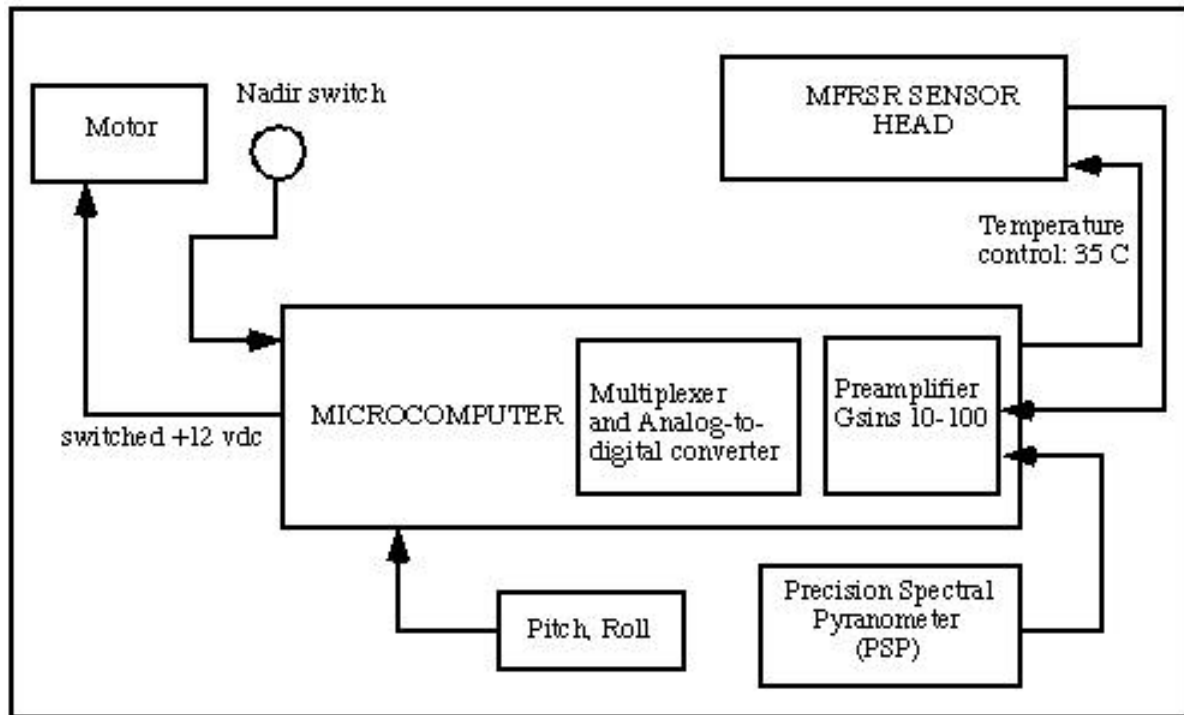
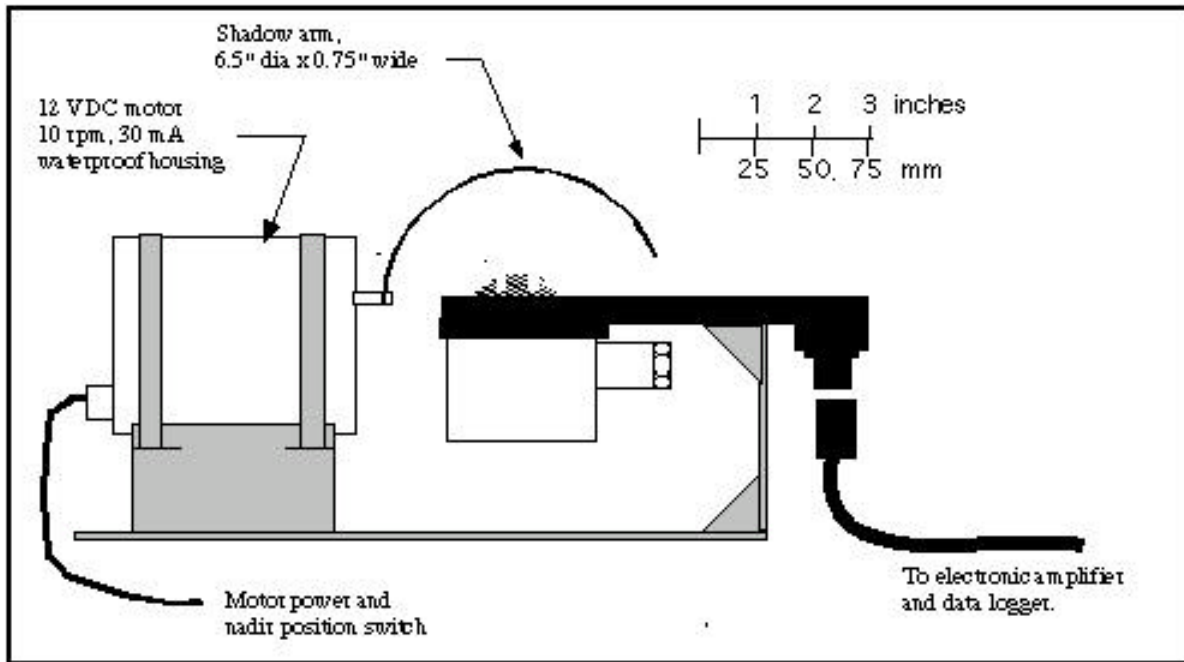
The stock head must be modified to decrease the response time of each of the seven



Figure 1: The PRP mounted on the R/V *RON BROWN* during the GasEx '98 experiment in May-June 1998. The data logger is located under the plate on the diagonal strut in this photograph.

channels to about one millisecond. The responses of the silicon cell detectors are well below one millisecond, but the internal preamplifiers in the stock head are too slow. For the first prototype head, the preamplifier gain resistors were reduced by a factor of 10. Special second-stage preamplifiers in the data logger compensated for the reduced output. The modification was easily made and laboratory tests showed that it added no additional noise to the measurement. (Yankee Environmental Systems has suggested that by reducing the filter capacitors we can speed the preamplifiers without sacrificing gain and this will be done to future heads.)

The FRS spectral radiometer data logger is custom-made and packaged in a waterproof housing that resides in close proximity to the PRP (Figure 1). The low-power microprocessor computer, a Tattletale Model 8 by Onset Computer Company, has the power to accommodate a sophisticated program in a remote package. Using a Motorola 68332 microprocessor, it has a 500 Kbps RS-232 interface and a tunable system clock from 160 KHz to 16 MHz. It programs in C and has a PIC 16C64 microcontroller which operates as a super-controllable clock, and provides improved external bus expansion, a precision real-time clock, and increased memory as required. It weighs only one ounce and can draw less than 250 μ A in low power mode. The data logger incorporates radio interference and surge protection, operates over a -40 to 65°C temperature range, and is waterproof and immune to shock and vibration.



North
East
South

Figure 2: Mechanical sketch and electronic block diagram of the Portable Radiation Package.

The PRP data logger has eight analog input channels with preamplifiers. The overall gain for each channel is adjusted to provide near full scale voltage (typically 4000 mv) to the analog-to-digital converters if the head is directed at the solar beam on a clear day. The 12-bit analog-to-digital converter noise figure is ± 1 bit, which converts to a measurement resolution of approximately ± 1 mv or 0.05% of full scale. All eight channels can be converted in a few milliseconds, well within the 10 ms sampling period for each channel.

The spectral radiometer head, PSP, and other required analog signals number greater than eight and compromise had to be made for this prototype. Duly, only six of the FRS spectral radiometer channels could be recorded and the 960 nm channel was omitted. Future PRP designs will have added analog-to-digital converter input and will accommodate all detector channels.

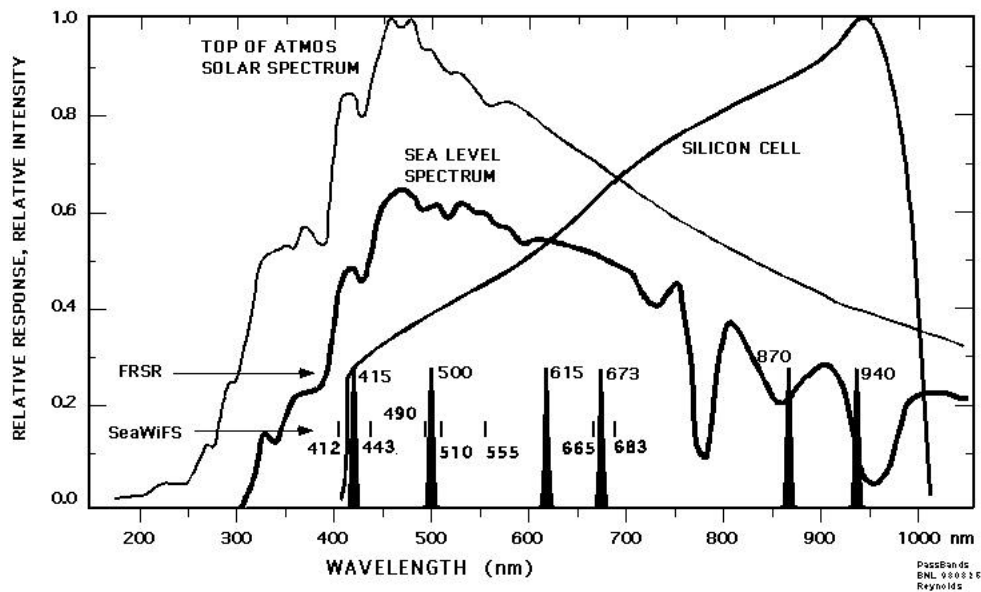


Figure 3: Typical spectra of solar radiance at the top of the atmosphere and at ground level shown with response curves for a standard silicon-cell photodiode, the equalized International Light silicon-cell sensor, and the Eppley thermopile sensor using a Shott glass dome as the filter.

2. Sweep Analysis and Block Averaging

In operation the FRS spectral radiometer arm rotates continuously. A magnetic reed relay tells the controller when the arm is at its nadir position. The controller measures the time between consecutive nadir crossings and computes the rotational speed. During a full rotation a sequence of operations and decisions is performed. Figure 4 shows the sequence of events over the course of one revolution. Sweep time is recorded at the instant of nadir crossing (N) and this marks the beginning of a sweep.

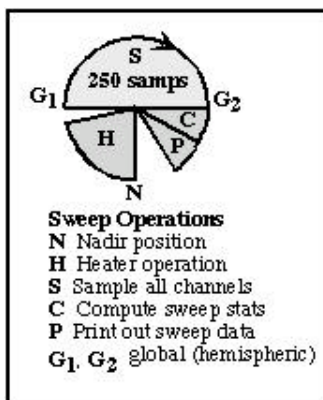


Figure 4: The sequence of operations as the shade arm makes a cycle around the sensor.

The first quarter revolution (H) is used to heat the sensor head. The head is maintained at a temperature of 40°C. Keeping the head at a constant temperature above ambient reduces condensation inside and on the diffuser, and minimizes thermal stresses on the silicon-cell filters. [It has been determined that a calibration shift occurs when the filter material de-laminates from the surface of the photodiodes. Temperature cycling exacerbates the delamination process. (Mark Beaubean, Yankee Environmental Systems, personal communication)]. The head is well insulated and has a 25 W heater circuit. Thus, the heating current is applied only when needed, which reduces system power requirements. The heating current is suspected of affecting the preamplifier output, and so is not applied during the sampling. The heater is turned off just before the arm reaches the sensor horizon.

The “sweep” (S) is the sequence of measurements that are made during the passage of the arm over the upper hemisphere. At the beginning of the sweep (G₁) the computer measures the pitch and roll of the sensor, then begins making analog-to-digital conversions. During the sweep, 250 samples of each channel, a 100 Hz sampling rate, including the Eppley PSP, are taken. At the end of the sweep (G₂), a second set of pitch and roll measurements is made.

In the last quarter of revolution, the sweep data are analyzed (C) and a brief message is sent to the base station computer (P). Full sets of sweep data are stored in the logger. At the end of one minute, the arm is stopped at its nadir and a compressed binary packet of all sweep data is sent to the base computer, which is usually a laptop PC running special packet reception software. Once the packet has been transmitted, the arm begins again. The serial data rate is 19200 bps and the arm is halted only a second or two.

During the sweep analysis period (C), the data logger processes each sweep. Only raw

voltages are considered during the analysis. Calibration coefficients are applied in post analysis and only at the end of all signal processing. The first step in sweep processing is computation of hemispheric (global) irradiance. The first and last five samples of each sweep are averaged. These samples occur when the arm is at the horizon relative to the sensor. We refer to these measurements as G_{i1} and G_{i2} where $i = 1, \dots, 6$ are the channels of the sensor head.

Next, the data logger determines if a significant shadow is present. Only the broadband channel is used for this decision. The “shadow ratio” is a sensitive measure of the intensity of the direct solar beam and is computed by the equation

$$\epsilon = \frac{v_{av} - v_{min}}{\sigma_v} \quad (1)$$

where v_{av} is the mean signal voltage for the entire sweep, v_{min} is the minimum signal voltage, and σ_v is the standard deviation for the sweep. It has been found that a criterion of $\epsilon \geq 2.3$ captures almost all true shadow cases and seldom permits a false positive. The integer i_{min} marks the position of v_{min} in the 250-element sweep array.

When $\epsilon \geq 2.3$, a sweep is deemed to contain a significant shadow and it is analyzed, block averaged, and stored in the binary packet array. Block averaging of the sweep retains all of its significant characteristics but significantly reduces data storage requirements. Block averaging begins at index i_{min} and moves left and right through the sweep array. Twenty-three contiguous block averages, b_{ij} where i is the channel number 1–6 and j is the bin number, are computed according to the table below.

Table 1: Table of sweep block averaging bins, $b_i(j)$, $i = 1 \dots, 23$, $j = 1 \dots 6$. The 23 bins and the number of points in each bin are shown. Bin 12 has only one point, the minimum (shadow) point.

1	2	3	4	5	6	7	8	9	10	11	12	13	14	15	16	17	18	19	20	21	22	23
30	20	20	10	10	10	5	5	5	5	5	1	5	5	5	5	5	10	10	10	20	20	30

The shadow index, i_{min} , can occur anywhere in the 250-point sweep array. Thus, in the block averaging process some bins will fall outside the sweep. Those bin averages are set to “missing.” The block average array for each channel 1–6 and the PSP data are stored in the logger and transmitted to the base PC at the end of each minute. A transmission on a sunny period would have about 2500 characters and with no shadow 400 characters. All the data for a sunny day take approximately 1.5 MB.

2.1. Sweep Averaging

At present, defining the appropriate timing variables for sweep averaging has been determined empirically. The procedures for analyzing the FRS spectral radiometer data were developed for the SeaWiFS cruise on the R/V *Bellows* and are described below. The binary packets are collected and stored in the base computer. A decompression program produces a set of ASCII data files that are processed using Matlab procedures for averaging and plotting.

Individual, bin-averaged sweep data have too much variability to be of use for sun photometry because of the motion of the ship. Smoothing of the time series is required. A smoother that would minimize measurement uncertainty yet preserve sufficient resolution for analysis was investigated. Emphasis was placed on the rather uncomplicated situation of a clear

direct solar beam with partly clear or clear sky. Clouds will alter the integrated diffuse irradiance on a time scale that is slow compared to the averaging times considered, as long as they do not block the direct beam. Simple averages over a two-minute period, 22 sweeps, were found to reduce the noise by a factor of approximately 4.7, yielding worst-case measurement uncertainties of 8-9 Wm^{-2} for the hemispheric and less than 1 Wm^{-2} for the shadow value.

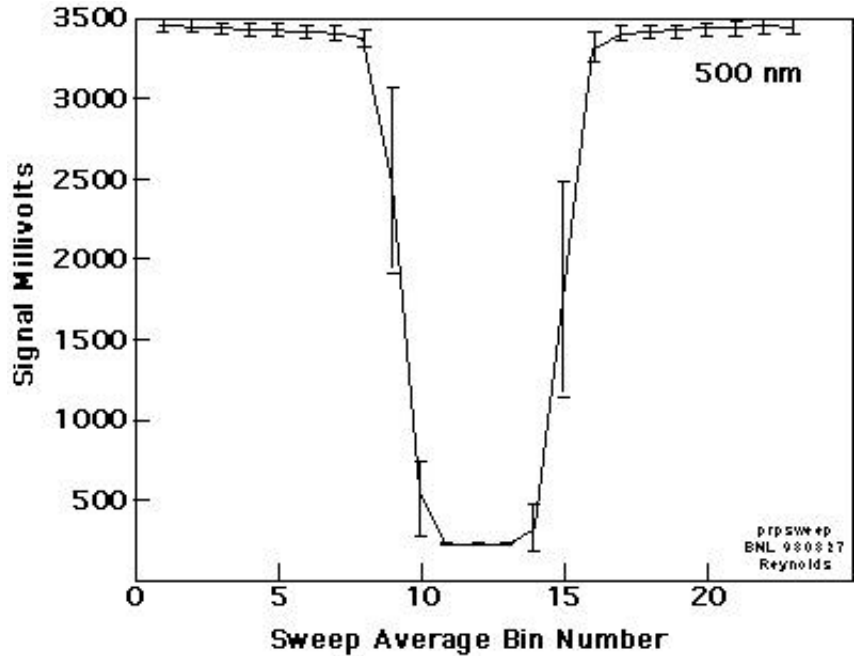


Figure 5: A two-minute average of 20 sweeps from the 500 nm channel on a sunny day (980403) taken on the R/V *Bellows* cruise to the Bahama Islands. The vertical bars indicate the standard deviation in the measurements for each bin. Note that the shadow values, with no direct beam component, have exceptionally low variability. Likewise, the shoulder value variability is small, indicating that the combined bin averaging and two-minute averaging are quite effective at reducing motion-induced noise.

An example of the effectiveness of the two-minute averaging process is shown in Figure 5. The figure is a plot of two-minute mean values with standard deviation bars for all 23 bins of the 500 nm channel on a typical sunny day period. The global values have a variability of about 100 mV (3%) while the shadow value variability is negligible.

Three measurement quantities are selected from the mean sweeps. The global irradiance, G_i , for spectral channels $i = 1-6$ has a sample period of 2.25 sec as discussed above. The shadow value, $S_i = b_i(12)$, is the minimum voltage measured in the sweep. The edge, or shoulder, value is given by

$$E_i = 0.5(b_i(7) + b_i(17)) \tag{2}$$

where $b_i(7)$ and $b_i(17)$, are sweep block average bins that are always outside the shadow region yet close to the disk of the sun. The edge value is a close approximation to the global irradiance less the amount of sky removed by the arm in the vicinity of the sun.

Figure 6 is an example of two-minute data for one day during the SIMBIOS cruise on the R/V *Bellows* to the Bahamas. A theoretical computation of the clear sky surface radiation

(a) based on an estimated integrated water vapor value of 3 cm matches the global irradiance values (b) well. The edge values (c) are shown as two curves representing mean plus and minus one standard deviation for the two-minute average. Finally, the shadow values (d) are typically 8% of the peak global value and are quite sensitive to the amount of cloud. The decomposition of the solar flux into the direct beam component into a horizontal plane, H_i , and the diffuse component, D_i , then is

$$D_i = S_i + (G_i - E_i) \quad \text{and} \quad (3)$$

$$H_i = E_i - S_i \quad (4)$$

for any spectral channel, i .

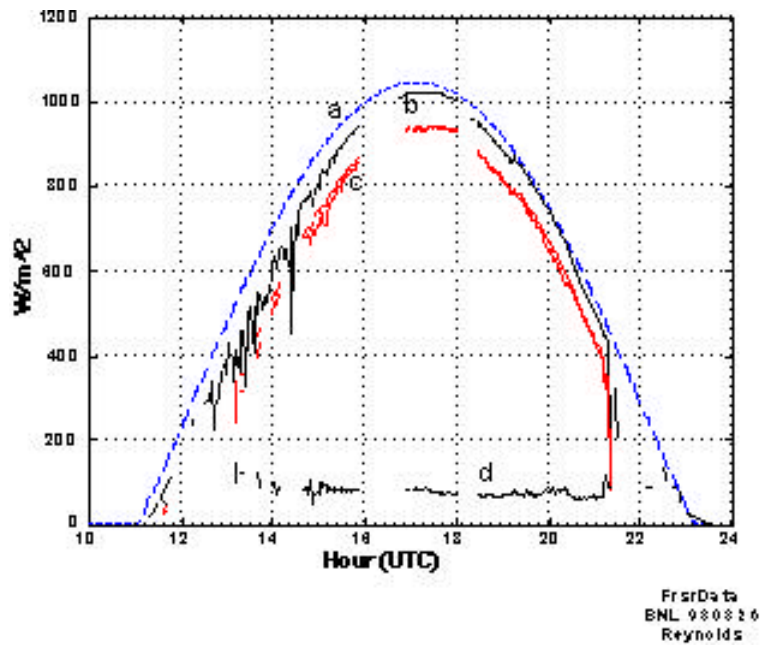


Figure 6: Example of data from the R/V *Bellows* cruise in 1998, JD092. (a) Theoretical clear-sky irradiance on a horizontal plane, (b) measured broadband irradiance, (c) direct-beam irradiance on a horizontal plane (the mean plus and minus the measurement standard deviation is shown as two curves), and (d) the diffuse (sky) component.

2.2. Calibrations

For the SIMBIOS measurements, the FRS spectral radiometer head was calibrated by Yankee Environmental Systems, a certified calibration facility. The standard spectral radiometer calibration produces three products. The first calibration product is a linear, direct normal irradiance gain equation with units of $\text{mv}/(\text{Wm}^{-1})$ for the broadband channel and $\text{mv}/(\text{Wm}^{-1}\text{nm}^{-1})$ for the narrowband channels. These calibration equations are corrected for the individual band-pass spectral responses for the head. The second calibration product is the bandpass spectral responses for the narrowband channels. The narrowband response for the SIMBIOS head is shown in Figure 7. Finally, the zenith angle correction is measured on two planes, one on a south-to-north plane (the head connector points to relative north on the head) and one on a west-to-east plane. The zenith angle corrections are shown in Figure 8.

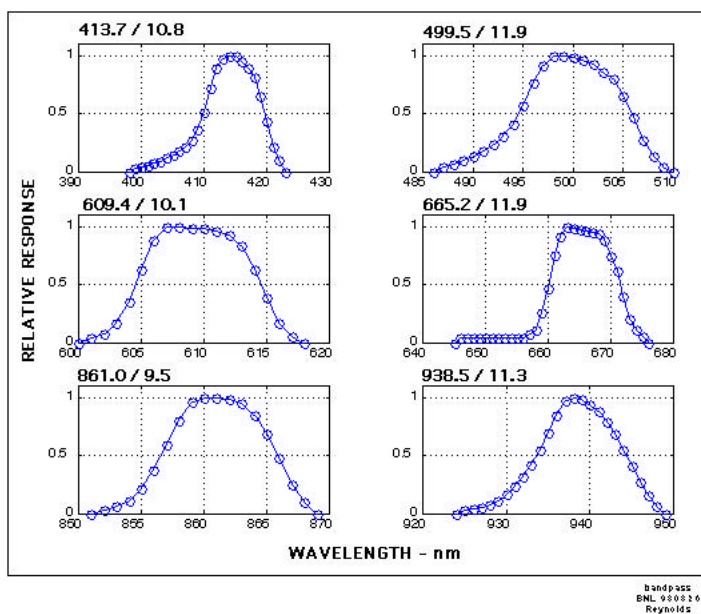


Figure 7: The band pass response for FRS spectral radiometer head F486 as calibrated by Yankee Environmental Systems, May 1998. The equivalent bandwidth of each channel is the width of a top hat window with the same area as the response curve. The center frequency of the channel is the point of maximum response.

The preamplifiers in the FRS spectral radiometer data logger were carefully calibrated in the laboratory using precision millivolt reference sources and voltmeters. The voltage gain data were combined with the direct normal head calibration coefficients for a single calibration equation relating radiation to analog-to-digital conversion counts (equivalent to millivolts). A straight line, linear equation adequately describes the calibration results.

$$\text{irradiance} = C_{i1}V + C_{i2} \tag{5}$$

where the C_{i1} and C_{i2} convert the millivolt measurement to the equivalent radiation units.

Users of the spectral radiometer head have registered a great deal of consternation over the fact that the head calibration factors are known to vary over time. The bandpass and zenith angle correction terms do not exhibit this deterioration, but the gain term, C_{i1} , can drop to

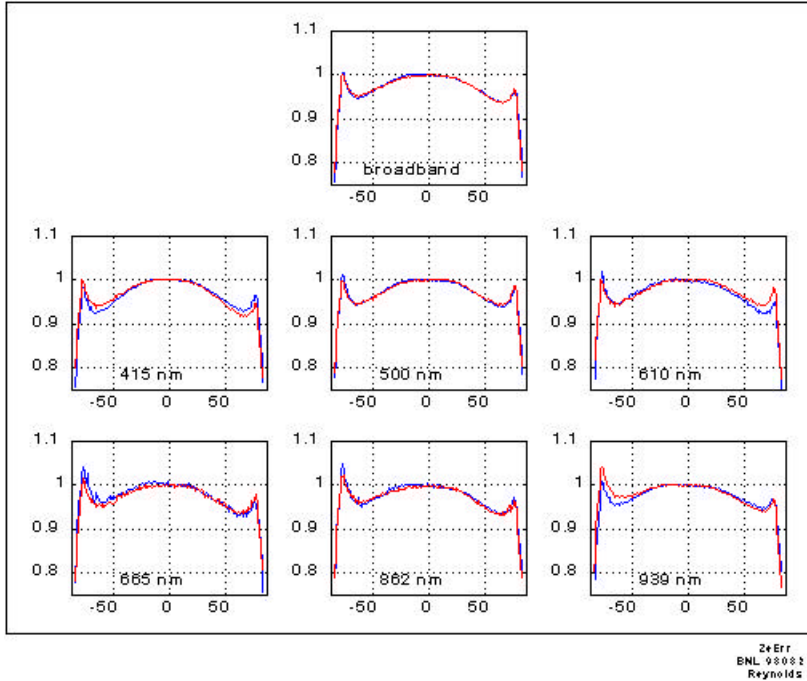


Figure 8: The zenith angle response for each channel of head number F486. Zenith angle error is measured by rotating the sensor in orthogonal directions, E-W and N-S. The two curves track closely, but diverge somewhat (0.5%) at angles greater than 60°.

as much as one half its original value due to a de-lamination of the filter layers. The effect is most pronounced in the 655 and 683 nm channels, but it appears that aging helps stabilize the process. The SIMBIOS head has been well aged, and the opinion from Yankee is that we should see excellent long-term performance from this unit. Regular factory calibrations and field comparisons should show up any future filter drift.

The direct beam irradiance on a horizontal plane, H_i , is converted to a direct beam irradiance into a normal plane with the equation

$$N_i = \frac{H_i}{\chi(\zeta) \cos \zeta} \quad (6)$$

where H_i is computed in millivolts using equation 4, ζ is the solar zenith angle, χ is the zenith angle correction, and i is the channel number. The zenith angle is computed using a solar ephemeris program that requires geographic position and time. For the R/V *Bellows* cruise, position was provided by a separate GPS and data logger system that was co-located with the PRP. The zenith angle correction terms, χ_i , were derived from the head calibration tables shown in Figure 8. In this study, we were concerned with measurements for zenith angles less than 60°. Also, our compass failed and the R/V *Bellows*, being a simple ship, was not recording its position, course, or azimuth. Thus, for the purposes of this study, the 14 curves of Figure 8 were combined into a single curve that was symmetrical around zero. A polynomial equation was fit to the data and the agreement was good for all azimuth angles and for zenith angles from 0–60°.

The computer value for N_i includes zenith angle corrections that were present in the global measurements. Therefore, as a next step, corrected values for H'_i and global irradiance,

G'_i , in millivolts, are computed by

$$H'_i = N_i \cos \zeta \quad (7)$$

$$G'_i = H'_i + D_i \quad (8)$$

As a last step, corrected irradiance values are converted from engineering units to physical units with the calibration coefficients as described in equation 5.

3. Conclusions

The Portable Radiation Package (PRP) with its Fast Rotating Shadowband (FRS) spectral radiometer was developed for making long-term, routine, downwelling radiation measurements from moving platforms such as ships. The design, described in this paper, and results from a SeaWiFS SIMBIOS cruise to the Bahamas, described in the cruise report and data report that are attached papers, demonstrate the effectiveness of the FRS for sun photometric measurements.

During the next year we expect to produce considerable field data from this and other PRP systems presently under construction. Extensive testing of the instrument using a pitch-roll table on land sites, at-sea intercomparisons, and long-term shipboard data sets is expected to set bounds on the usefulness of the PRP in different ocean settings and platforms.

4. References

Harrison, Lee, Joseph Michalsky, and Jerry Berndt, Automated multifilter rotating shadow-band radiometer: an instrument for optical depth and radiation measurements, *Applied Optics*, 33, 5126–5132, 1994.

Harrison, Lee and Joseph Michalsky, Objective algorithms for the retrieval of optical depths from ground-based measurements, *Applied Optics*, 33, 5126–5132, 1994a.

Guzzi, Rodolfo, Gian Carlo Maracci, Rolando Rizzi, and Antonio Siccardi, Spectroradiometer for ground-based atmospheric measurements related to remote sensing in the visible from a satellite, *Applied Optics*, 24, 2859–2864, 1985.

Wesely, Marvin L., Simplified techniques to study components of solar radiation under haze and clouds, *Jour. Appl. Meteor.*, 21, 373–383, 1982).

5. Acknowledgements

This development is symbiotic with efforts of the U.S. Department of Energy Atmospheric Radiation Measurement Program Ocean Project (AOP) to produce long-term time series of radiation at the air-sea interface. Special thanks go to Scott Smith and Ray Edwards of Brookhaven National Laboratory who provided mechanical and electronic expertise and support. Steve Boose of BNL designed the microprocessor electronics.